Hindawi
Journal of Applied Ichthyology
Volume 2023, Article ID 6650863, 13 pages
https://doi.org/10.1155/2023/6650863

Research Article

Acoustic Target Strength of Jellyfish, *Nemopilema nomurai*, Measured at Multi-Frequency and Multi-Orientation

Hang Yang,[1,2] **Jing Cheng**,[2] **Taolin Tang**,[2] **Jun Chen**,[2] **and Guodong Li**[2]

[1]*College of Engineering Science and Technology, Shanghai Ocean University, Shanghai 201306, China*
[2]*Fishery Machinery and Instrument Research Institute, Chinese Academy of Fishery Sciences, Shanghai 200092, China*

Correspondence should be addressed to Guodong Li; liguodong@fmiri.ac.cn

Received 18 July 2023; Revised 10 October 2023; Accepted 14 October 2023; Published 23 October 2023

Academic Editor: Mohamed Abdelsalam

The jellyfish *Nemopilema nomurai* occupies an important position in the Northwest Pacific ecosystem, and monitoring its biomass is necessary to ensure the protection of fishery resources and the safety of offshore industrial production. The acoustic method has been proposed for jellyfish flux estimation and bloom warning, in which the target strength (TS) of the jellyfish is a crucial parameter. However, varied swimming orientations of jellyfish aggregation result in different backscatter strengths. The acoustic echo characteristics in horizontal swimming orientations and multi-frequency broadband signals are yet to be revealed. This study aims to obtain the TS of jellyfish in various orientations and to comprehensively investigate the jellyfish acoustic echo features at various frequency broadband sounds. In an anechoic tank, we used wide-band echosounder and 70 kHz, 120 kHz, and 200 kHz split-beam transducers to measure the TS of jellyfish swimming omnidirectionally. The results show a difference of approximately 4 dB in the jellyfish's normalized TS at 70 kHz (frequency range: 45 kHz to 95 kHz) and 200 kHz (frequency range: 160 kHz to 260 kHz) center frequency. The normalized TS of jellyfish varies by around 8 dB between horizontal and vertical swimming orientations. For jellyfish swimming horizontally, the TS and bell diameter have the following least squares fits: $TS_{D70kHz} = 20\log D - 89.36\,(r^2 = 0.83)$; $TS_{D200kHz} = 20\log D - 93.85\,(r^2 = 0.83)$. The swimming orientation has significant effects on TS estimation and model construction.

1. Introduction

Jellyfish belong to coelenterates, one of the most significant groups of marine organisms, and they play an essential role in maintaining the marine ecosystem [1]. In recent years, jellyfish populations in the Northwest Pacific Ocean, particularly those along the eastern coast of China and in the seas of Korea and Japan, have shown an upward trend [2–4]. The typical jellyfish species in the Northwest Pacific Ocean include *Rhopilema esculentum*, *Nemopilema nomurai*, *Cyanea nozakii*, and *Aurelia aurita* [5]. The proliferation of giant jellyfish such as the *Nemopilema nomurai*, the dominant species in the Northwest Pacific Ocean in summer [6], has caused adverse effects on fishery production in the region. Jellyfish outbreaks have led to frequent reductions in fishery catches and damage to fishing gear [7–9]. The sudden aggregation of jellyfish poses significant threats to the safe operation of circulating water cooling systems in coastal nuclear power plants, causing short-term physical damage [10]. Furthermore, their aggregation seriously endangers industrial production safety [11, 12]. Related studies have found that climate changes such as dissolved oxygen in marine waters [13], temperature, wind direction [14, 15], and human industrial activities [16] are complexly associated with the population growth and outbreak of jellyfish, which increases the uncertainty of jellyfish outbreaks.

Scholars have conducted much research aimed at minimizing the risks and effectively tracking changes associated with jellyfish blooms. Among various techniques, acoustic survey techniques have been considered essential for quantitatively assessing target organisms and issuing disaster warnings in recent years [17, 18]. Hydroacoustic techniques enable noncontact detection while preventing targets from being damaged by net fishing [19] in

comparison to semiquantitative estimating techniques like net sampling [20] and visual monitoring [21]. The method is based on determining the target organism's volumetric scattering strength in conjunction with individual organisms' target strength (TS) to determine their resource density [22]. Measuring the individual TS of target species is one of the initial steps necessary for hydroacoustic surveys, which establishes the foundation for ascertaining the connection between the scattering strength of target animals and the resource density [23].

The acoustic properties of marine creatures, including those with swim bladders, have been extensively studied using acoustic techniques like in situ and ex situ TS assessments [24–28]. However, as weak scatterers with variable morphology, jellyfish still need to be adequately characterized acoustically. Previous studies have been conducted on the acoustic properties of certain jellyfish species, including ex situ measurements of TS and the impact of pulsation on the TS of sand jellyfish [29], models of target strength in vertical swimming posture [30], and analyses of the acoustic characteristics of various jellyfish species, including *Nemopilema nomurai*, *Cyanea nozakii*, and *Aurelia aurita*, at various frequencies [31]. However, the majority of the investigations on the acoustic properties of jellyfish have utilized point frequency or narrowband measurement systems at 38 kHz and 120 kHz. Broadband measures are being employed more frequently as a result of the advancements in hydroacoustic broadband technologies [32]. Broadband measurement systems utilizing pulse compression techniques offer superior distance resolution and peak instantaneous signal-to-noise ratio compared to narrowband systems [33]. They also enable a spectral analysis of TS and identification [34]. Studies on the acoustic characteristics of jellyfish in multiple frequency bands under broadband conditions are yet to be reported. In order to determine if jellyfish TS models based on narrowband and single frequency signals can be directly applied to broadband acoustic surveys, jellyfish TS data measured using broadband signals must be gathered.

Additionally, the current measuring approach and TS model only consider data regarding the jellyfish's vertical swimming direction. Studies on the transport and swimming mechanics of jellyfish have demonstrated that during jellyfish aggregation blooms, jellyfish move in complex patterns like vertical aggregation and horizontal swimming [35, 36]. Hydroacoustic transducers are also positioned differently in practical applications to achieve a more comprehensive monitoring range, such as horizontally or downward [37]. Changes in the target's angle concerning the transducer will undoubtedly result in significant changes in the acoustic reflection cross section, impacting the overall TS assessment and the abundance estimation. Although acoustic measurement experiments can better reflect the TS of jellyfish under realistic environmental conditions, the sample size is also an important factor limiting the accuracy of the obtained TS models. Therefore, it is significant to establish a physical model of acoustic scattering of jellyfish *Nemopilema nomurai* to understand the TS of jellyfish under more bell diameters [38]. The distorted-wave Born approximation model (hereafter DWBA model) was initially applied to TS studies of weak scatterers such as shrimps [39, 40]. The connection between TS and the biological properties of jellyfish has also recently been investigated using the DWBA model [38]. The expansion of sample size based on the DWBA model is made possible by the DWBA model's ability to represent well the variation of TS with measurement angle [41]. There are fewer basic studies on the backscattering characteristics of jellyfish compared to other marine organisms like swim bladder fish, particularly on measuring TS in multiple frequencies and attitudes based on hydroacoustic broadband signals, and the current jellyfish acoustic models still need to be improved.

Therefore, the objective of this study is to obtain the backscattering characteristics of jellyfish *Nemopilema nomurai* at different swimming orientations and detection frequencies by utilizing a broadband split-beam measurement system and to estimate the relationship between TS and bell diameter of jellyfish at different swimming orientations.

2. Materials and Methods

2.1. Sampling and Testing System Construction. A research vessel collected multiple jellyfish *Nemopilema nomurai* in October 2022 from the free-floating jellyfish in the upper layers of the East China Sea. The sampling sites are shown in Figure 1. These jellyfish ranged in size from 7 cm to 32 cm in bell diameter and weighed from 14 g to 2200 g in their natural state. Each specimen underwent a visual examination to ensure that no other organisms were affixed to its surface and that its body was unharmed and free of air bubbles. Individuals in standard form were immediately selected and carefully transferred to a seawater tank to facilitate subsequent TS measurements in the anechoic tank.

In an anechoic tank measuring 11 m ∗ 7 m ∗ 6 m (Figure 2), we constructed a jellyfish acoustic measurement system in November 2022. On one side of the tank, the measurement device was fixed on crane A and placed 2 meters underwater. A metal rod is installed under crane B on the other side of the anechoic tank to hold the measurement target. The rod is fixed to the crane's rotating mechanism, which can be moved through a predetermined number of degrees. An underwater camera has been installed on the anechoic tank's side to keep track of the angle and condition of the jellyfish. The test used broadband echosounders (EK80) and three split-beam transducers with the models and frequency range shown in Table 1. Prior to the experiment, the anechoic tank's water temperature and salinity parameters were measured using a portable water quality analyzer (YSI-Professional Plus) to calculate the absorption coefficient and obtain parameters such as sound speed. The water temperature was 13.7°C, and the salinity was 25.73 ppt. The initial settings of the hydroacoustic transducers were then set accordingly. Table 1 shows the specific settings of the three transducers.

The measurement system was calibrated using a 38.1 mm tungsten carbide standard sphere before the experiment and again at the end [42]. In addition, the near-field ranges

Figure 1: Map of sampling sites.

corresponding to the three transducers were calculated to ensure that the target was outside the near-field range of the transducer for high measurement accuracy. According to the following formula [43]:

$$R_C = \frac{\pi D^2}{4\lambda}, \tag{1}$$

where λ is the wavelength and D is the diameter of the transducer. The diameters of the active portions of the ES70-C, ES120-C, and ES200-C transducers are 250, 160, and 100 mm, respectively, which correspond to a near-field range of 2.34 m, 1.64 m, and 1.07 m. The experiments ensured that individual jellyfish were outside the sonar's near-field range of the sonar when conducting TS measurements.

2.2. Measurement of Individual TS and Parameters. The jellyfish TS measurements were carried out in a large seawater anechoic tank (Figure 2). Two jellyfish samples died before the experiment but maintained their intact forms. We placed them in the tank for quick measurements. Since the actual swimming state of jellyfish in seawater consists mainly of horizontal and vertical movements [35, 36], the transducer was arranged horizontally rather than in the usual longitudinal way for this experiment to obtain accurate TS at different angles. We first investigated the jellyfish fixation scheme to maintain the jellyfish at the desired angle to the transducer. In this regard, two 0.128 mm monofilament lines were suspended from a metal rod under crane B, each with a 35 g counterweight block at the bottom for target positioning, to keep the jellyfish in a stable attitude during the test. A 0.128 mm diameter monofilament line was run through the ends of the jellyfish's bell and secured to the monofilament lines on each side (as shown in Figure 2) to keep the jellyfish with its bell facing the transducer. The monofilament line used for the experiments was made of polyethylene, which minimized the reflective TS of the line while meeting the weight-bearing requirements. The fixed line and system were also subjected to TS measurements prior to formal jellyfish measurements to ascertain that the backscattered strength would not interfere with the jellyfish.

During the test, controlled lifting mechanisms were used to position the ES70-C, ES120-C, and ES200-C transducers at 2 meters underwater and 3.5 meters from the side and rear walls of the tank. In order to regulate the jellyfish to be measured within the beam at all times, the jellyfish is suspended from a metal crossbar, kept 2 m below the water's surface and 4.5 m from the transducer, and rotated to a fixed angle by a rotating mechanism. Assuming an attitude angle of 90 degrees with the jellyfish crown facing the transducer, TS measurements were taken at 5-degree intervals at positions ranging from 0 to 180 degrees of jellyfish attitude angle. Figure 3 shows the jellyfish at various suspension angles. The pulse duration and pulse interval for the three frequencies were set to 1.024 ms and 500 ms, respectively, due to the proximity of the transducer and the jellyfish under test. The jellyfish was stabilized at its placement angle for five minutes before collecting the acoustic echo data. The experiment was then repeated with the jellyfish positioning its side towards the transducer's direction. As observed by the underwater camera throughout the experiments, the jellyfish maintained the correct posture to follow the metal rod to the exact target angle. The results of measuring each jellyfish's wet weight and bell diameter at the end of each experiment are shown in Table 2.

2.3. Data Processing and Jellyfish Model Building. Since a jellyfish's bell diameter differs from that measured in air when submerged, according to Hirose et al. [41], the bell diameter of a jellyfish in water is 0.67–0.76 times the bell diameter unfolding in air. We calculated the bell diameter of a jellyfish in water, and the results are shown in Table 2. Echoview 11.0 and the postprocessing software for EK80 were used to process the acoustic data. Single target detection was utilized to read the TS values at each angle between 4 and 5 m, with the TS threshold set to −90 dB. Since we waited for sufficient time for the jellyfish to stabilize before recording the data, we read multiple TS data pings directly from the raw echo data file at each point. For the target strength data in the horizontal and vertical swimming orientations, the backscattered cross-sectional area was calculated according to (2), and the mean target strength was derived by finding the average backscattered cross-sectional area [44]. For more generalized results, we resampled the target strength data based on its frequency and frequency density by interpolation to obtain a normal distribution [45] to find the mean target strength value of each sample in both swimming orientations.

$$\overline{TS}_{\text{mean}} = 10 \log \overline{\sigma_{\text{bs}}}. \tag{2}$$

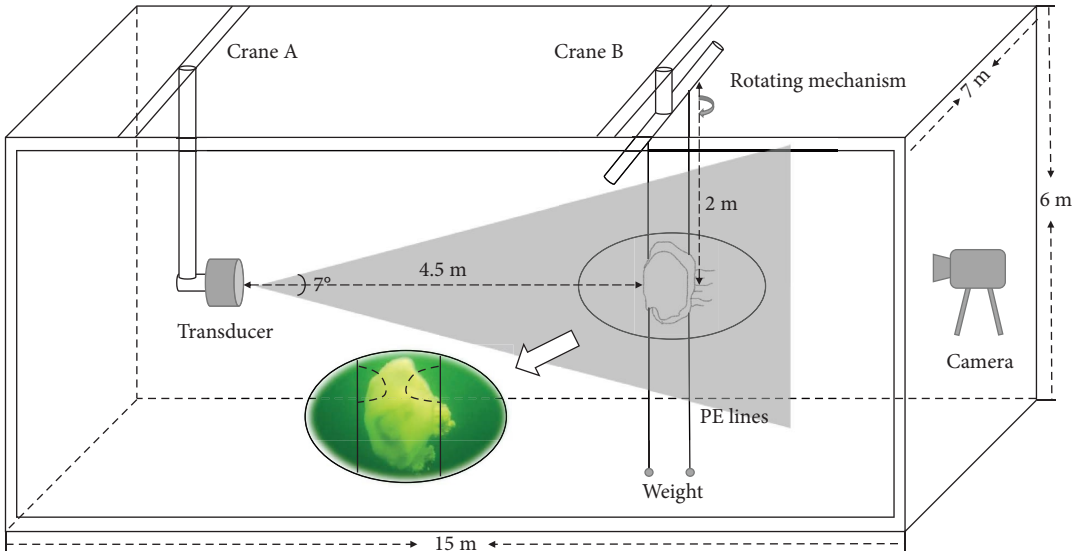

Figure 2: Schematic diagram of jellyfish target strength measurement. The cuboid represents the anechoic tank, and the four parallel lines on the top surface represent cranes A and B. The grey cylinder below crane A represents the hydroacoustic transducer. The rotating mechanism, specimen, and counterweight are shown below on the right-hand side of crane B. The grey area indicates the ideal beam range.

Table 1: Basic settings and parameters of EK80 series echo detector.

Transducer type	ES70-C	ES120-C	ES200-C
Diameter of transducer (mm)	250	160	100
Frequency (kHz)	70	120	200
Frequency range (kHz)	45~95	95~160	160~260
Power (W)	750	1000	1000
Beam type	Split beam	Split beam	Split beam
Beam opening angle (degree)	7	7	7
Range resolution (cm)	2 (chirp)	1 (chirp)	0.8 (chirp)
Sampling frequency (kHz)	20	20	20
Sound speed (m/s)	1470	1470	1470
Nearfield (m)	2.34	1.64	1.07

2.3.1. A Study of Jellyfish Target Strength Models Based on Measurement Angle. When measuring TS, which is directly related to the projected area of the point scatterer target within the beam, the measurement angle of a jellyfish within the beam is a crucial factor. For high-precision biomass measurements, it is crucial to investigate the connection between orientation changes and well-defined TS. The distorted-wave Born approximation (DWBA) model, one of the main TS models to study the relationship between the weak scatterer angle and TS, typically treats the target to be measured as a deformed cylinder with different diameters [39, 40]. It is primarily used to study acoustic scattering from three-dimensional objects with densities and sound velocities close to those of the surrounding medium. Since the jellyfish includes a bell-shaped body and tentacles and the body of the jellyfish is symmetrically and uniformly distributed along the centerline through its bell, it can be approximated morphologically as a combination of cylinders of different diameters.

$$f_{\mathrm{bs}} = \frac{k_1}{4}\int_{\vec{r}_{\mathrm{pos}}} a\left(\gamma_k - \gamma_\rho\right) e^{2i\vec{k}_2\cdot\vec{r}_{\mathrm{pos}}} J_1\left(2k_2 a\cos\beta_{\mathrm{tilt}}\right)/\cos\beta_{\mathrm{tilt}} \left|d\vec{r}_{\mathrm{pos}}\right|,$$

$$\mathrm{TS} = 10\log\left|f_{\mathrm{bs}}\right|^2. \tag{3}$$

The parameters involved in the distorted-wave Born approximation (DWBA) model are shown in Table 3.

γ_k and γ_ρ are the parameters determined by the sound velocity ratio h and density ratio ρ between the scatterer and the medium.

$$\gamma_k = \frac{1}{\rho h^2} - 1,$$

$$\gamma_\rho = 1 - \frac{1}{\rho}. \tag{4}$$

We chose a jellyfish individual with a bell diameter of 19 cm as the modeling sample. Before calculating the DWBA model, the underwater camera images of the measured jellyfish individuals were image-processed, and tracking profiles were created (as shown in Figure 4). The sound speed ratio $h = 1.0003$ and density ratio $\rho = 1.035$ were determined using the data from Hirose et al. [41] for individual jellyfish sound speed and density ratios, together with the bell diameter and wet weight of the selected individual jellyfish samples. The jellyfish were also considered to have the same sound velocity and density ratio if the measurement angle changed. Based on the theoretical

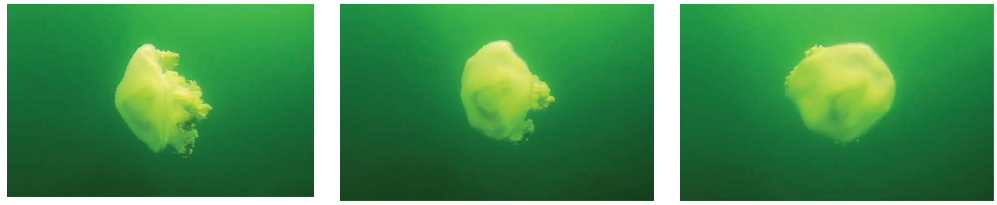

(a) (b) (c)

Figure 3: Individual morphology of jellyfish at different suspension angles. The jellyfish attitude angles are 0 degrees (a), 45 degrees (b), and 90 degrees (c), respectively.

Table 2: Diameter and wet weight of jellyfish samples.

Sample no.	Date	Bell diameter (cm)	Wet weight (g)
1	2022/11/29	7	14.6
2	2022/11/30	9	20.3
3	2022/12/01	19	1140
4	2022/12/02	29	1880
5	2022/12/03	32	2200

model, we divided the jellyfish into 300 cylindrical sections along the center line and built a DWBA model for the jellyfish *Nemopilema nomurai* at three frequencies based on the contour data.

2.3.2. A Study of Jellyfish Target Strength Models Based on Bell Diameter. Currently, classical jellyfish TS models are carried out in two dimensions, jellyfish bell diameter and wet weight, and the target strength models related to jellyfish bell diameter are

$$\mathrm{TS}_D = m \log D + b, \tag{5}$$

where TS_D is the backscattered TS, m and b are constants for a given species and frequency, and D is the bell diameter of the jellyfish [46].

First, we calculated correlation coefficients based on the measured jellyfish bell diameter (Table 2) and mean TS using linear regression analysis. The TS of jellyfish swimming in different directions was resampled 1000 times, and the mean TS was calculated. The relationship between jellyfish's average TS and bell diameter at different measurement frequencies and swimming directions was investigated separately.

3. Results and Discussion

The wet weight of the samples and the estimated bell diameter of the jellyfish in water are shown in Table 2, where the bell diameter of the jellyfish in its natural state in water ranged from 7 cm to 32 cm while the mass varied from 14 g to 2200 g. Five jellyfish samples underwent TS measurement in their horizontal and vertical swimming orientations, yielding over 74 TS datasets at each frequency for each sample. A total of 1110 sets of valid TS data were collected, among which Figure 5 illustrates the TS range for the horizontal swimming orientations of the jellyfish.

In the measured raw data, the jellyfish TS demonstrated a wide range of variability from −71 to −48 dB. Moreover, the variation in TS for a single jellyfish sample at a fixed frequency was also distinctly large, with factors such as swimming orientation, measurement angle, and pulsation motion contributing to the modulation of TS. Under consistent pulsation motion, the TS of 19 cm bell diameter jellyfish varied from 8 to 15 dB in the vertical and horizontal swimming orientation. The established DWBA model of jellyfish *Nemopilema nomurai* and the scatter plot of the measured data (Figure 6) showed that the maximum TS appeared in the vertical swimming direction of the jellyfish, while in the horizontal swimming orientation of the jellyfish, there was a large drop in the TS. By modifying the bell diameter parameters of the model, we simulated four jellyfish with different bell diameters in the range of 10 to 30 cm and obtained their average TS data in the horizontal swimming orientation.

After resampling the raw data, the frequency distribution of the TS was obtained (Figure 7). Assuming vertical downward detection, the mean TS of jellyfish with bell diameters ranging from 7 to 32 cm in the vertical swimming orientation was −67.8 to −51.32 dB (70 kHz), −72.7 to −56.3 dB (120 kHz), and −75.5 to −54 .9 dB (200 kHz). Using the same data processing method, we obtained average TS of −74.8 to −54.5 dB (70 kHz), −79.9 to −58.5 dB (120 kHz), and −80.1 to −60.1 dB (200 kHz) for the jellyfish swimming in horizontal orientation.

Based on the obtained mean TS, the optimal linear regression equations for the mean TS of the jellyfish in both directions were formulated with the jellyfish bell diameter. The mean TS displayed a positive correlation with the common logarithmic diameter (Figure 8). The optimal linear regression equation for the mean TS of the jellyfish in the vertical swimming orientation versus the jellyfish bell diameter is shown as equations (6)–(8).

$$\mathrm{TS}_{D70kHz} = 20 \log D - 83.24\left(r^2 = 0.84\right), \tag{6}$$

$$\mathrm{TS}_{D120kHz} = 20 \log D - 88.08\left(r^2 = 0.87\right), \tag{7}$$

$$\mathrm{TS}_{D200kHz} = 20 \log D - 90\left(r^2 = 0.83\right). \tag{8}$$

The best linear regression equations for the mean TS and jellyfish bell diameter in the horizontal swimming orientation of the jellyfish are shown as equations (9)–(11).

Table 3: Parameters of the DWBA model.

Parameter name	Parameter description
k	Acoustic wave number, $k = 2\pi/\lambda$
$\vec{r}_{pos}$	Position vector along the acoustic scattering axis
k_1	Number of acoustic waves in the medium
k_2	Number of acoustic waves in the scattering body
h	Sound velocity ratio
ρ	Density ratio
β_{tilt}	The angle between the cylinder and the incident wave at a given measurement angle
J_1	First-order Bessel functions of the first type
a	Radius of the cross section of the cylinder

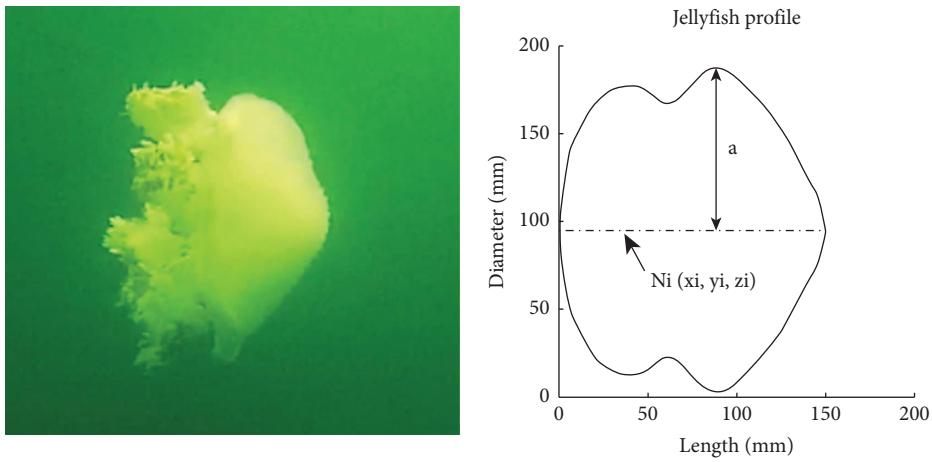

Figure 4: Jellyfish contour extraction. (a) A photograph of the jellyfish in the experiment. (b) The simulated outline of the jellyfish.

$$\mathrm{TS}_{D70kHz} = 20\log D - 89.36\left(r^2 = 0.83\right), \quad (9)$$

$$\mathrm{TS}_{D120kHz} = 20\log D - 93.74\left(r^2 = 0.82\right), \quad (10)$$

$$\mathrm{TS}_{D200kHz} = 20\log D - 93.85\left(r^2 = 0.83\right), \quad (11)$$

where D is the bell diameter of the jellyfish, TS_D is the TS at the corresponding frequency, and r is the correlation coefficient. From equations (7)–(11), it can be seen that overall, the average TS of the jellyfish is about 5 dB higher at 70 kHz than at 120 kHz, while the average TS values at 120 kHz and 200 kHz frequencies are close to each other and vary within 2 dB.

3.1. Differences in the Target Strength of Jellyfish in Different Frequency Conditions. For measuring the TS of the jellyfish *Nemopilema nomurai*, Kang et al. used narrowband signals at 38 kHz and 120 kHz, with mean TS varying from −59.2 dB to −41.2 dB at 38 kHz and −60.1 dB to −51.9 dB at 120 kHz [30]. The mean TS of the jellyfish *Nemopilema nomurai* ranged from −79.04 to −59.68 dB at 38 kHz and from −65.7 dB to −59.59 dB at 120 kHz in measurements by Hirose et al. [31]. The jellyfish also exhibited varying backscattering characteristics based on different detection frequencies. At 38 kHz and 120 kHz, measurements by Kang et al. revealed a 4 dB difference between jellyfish and those by Hirose et al. revealed a 4–6 dB difference [30, 31]. Figure 9 compares the jellyfish bell diameters of the similar specification jellyfish with the mean TS of the jellyfish at different frequencies and signal bandwidths. The results show that the test results of the similar specification jellyfish under a broadband signal with a center frequency of 120 kHz are close to those measured using a 120 kHz single frequency signal by Kang et al. [30] and Hirose et al. [31]. The jellyfish TS showed the same frequency-dependent fluctuations when measured using different broadband signals. The TS of jellyfish of the same size differed by 4-5 dB when measured using broadband signals with center frequencies of 70 kHz and 120 kHz, respectively, and their frequency difference characteristics closely matched those of Kang et al. when measured with a single frequency signal at 38 kHz and 120 kHz [30]. The results show that broadband signal measurements have similar characteristics to single-frequency signal measurements for TS measurements of a single target. However, because of the better distance resolution provided by pulse compression, the former may be more advantageous for future hydroacoustic surveys, especially for in situ measurements [28]. The different

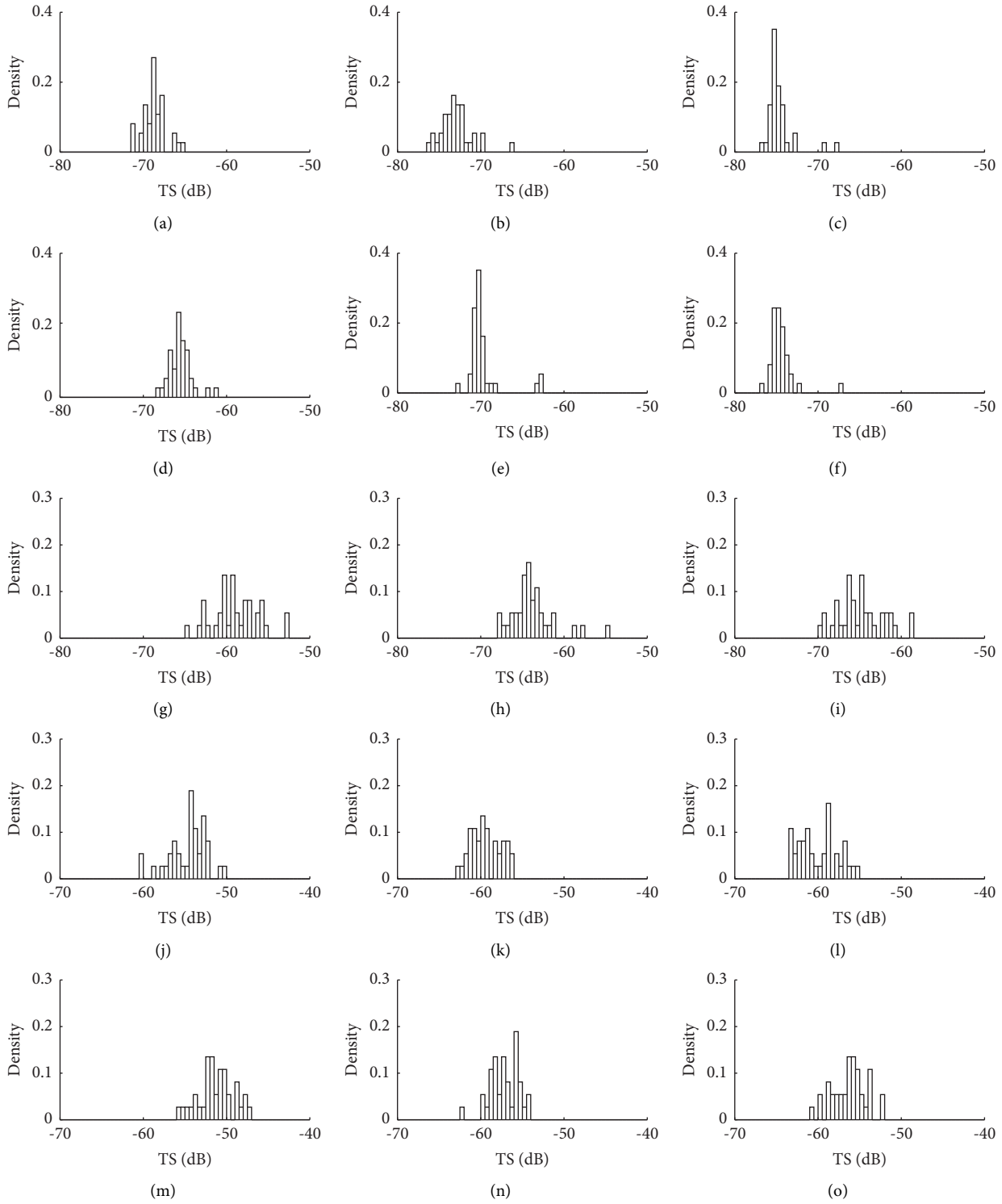

Figure 5: Histogram of target strength in the horizontal swimming orientation of each jellyfish at different frequencies. The caption of each subfigure is the number of the jellyfish sample-the center frequency of signals. The horizontal coordinate is the target strength, and the vertical coordinate is the probability density of the target strength measurements. (a) No. 1-70 kHz. (b) No. 1-120 kHz. (c) No. 1-200 kHz. (d) No. 2-70 kHz. (e) No. 2-120 kHz. (f) No. 2-200 kHz. (g) No. 3-70 kHz. (h) No. 3-120 kHz. (i) No. 3-200 kHz. (j) No. 4-70 kHz. (k) No. 4-120 kHz. (l) No. 4-200 kHz. (m) No. 5-70 kHz. (n) No. 5-120 kHz. (o) No. 5-200 kHz.

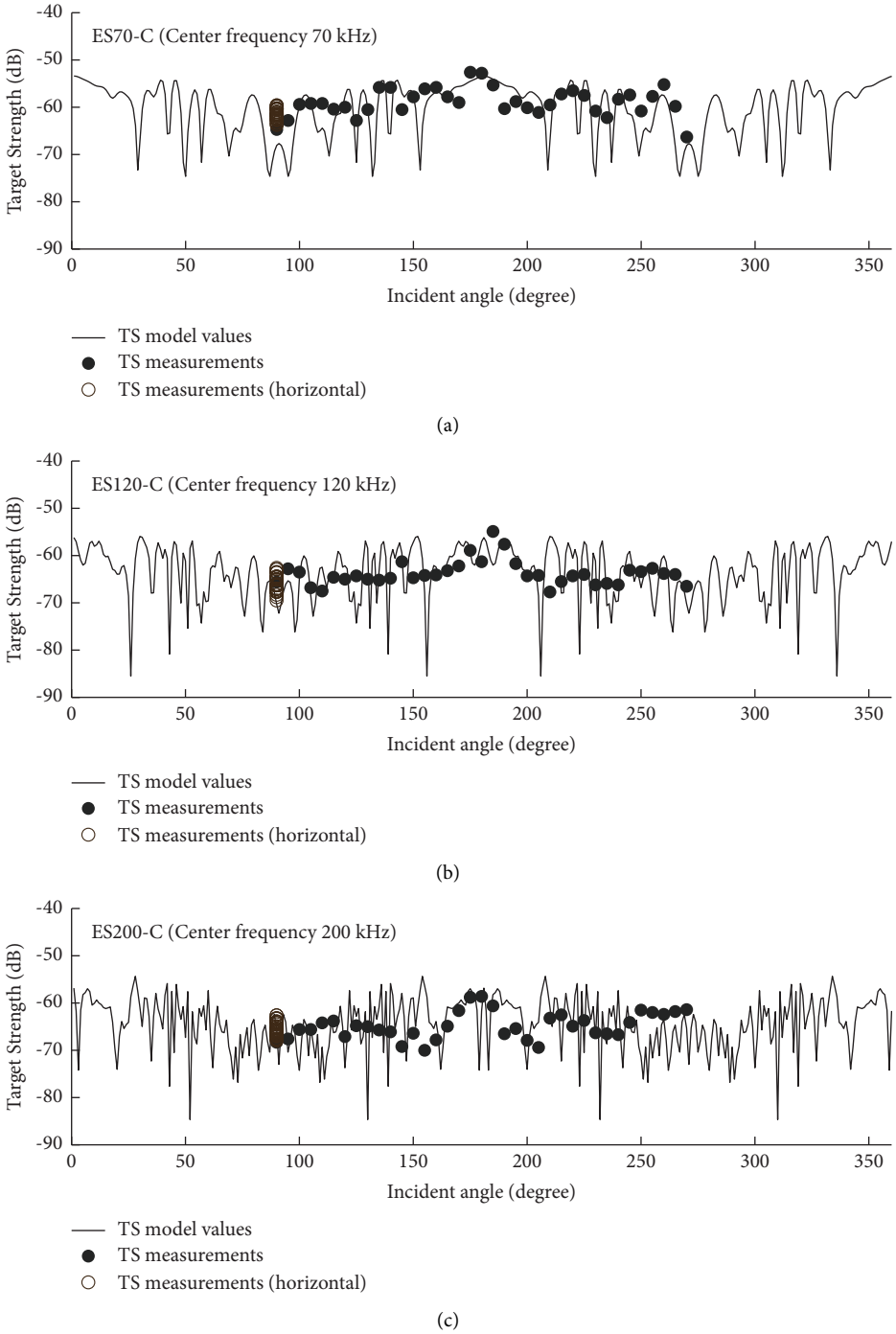

Figure 6: Relationship between incident angle and estimated TS of jellyfish DWBA model at different frequencies. The solid black lines represent the theoretical values for each angle of the model, while the solid black circles indicate the measured values, and the black hollow circles indicate the measured values (horizontal). The data corresponding to 180 degrees in the figure were obtained when the jellyfish was at an attitude angle of 90 degrees.

backscattering characteristics of jellyfish at different center-frequency broadband signals may provide more choices of detection bands for jellyfish biomass assessment and differentiate species based on these properties in resource survey assessments.

3.2. Differences in the Target Strength of Jellyfish in Different Swimming Orientations. Moreover, it is noteworthy to observe how the jellyfish's swimming orientation affects the TS. Figure 10 compares the mean target strength for different swimming orientations measured by broadband

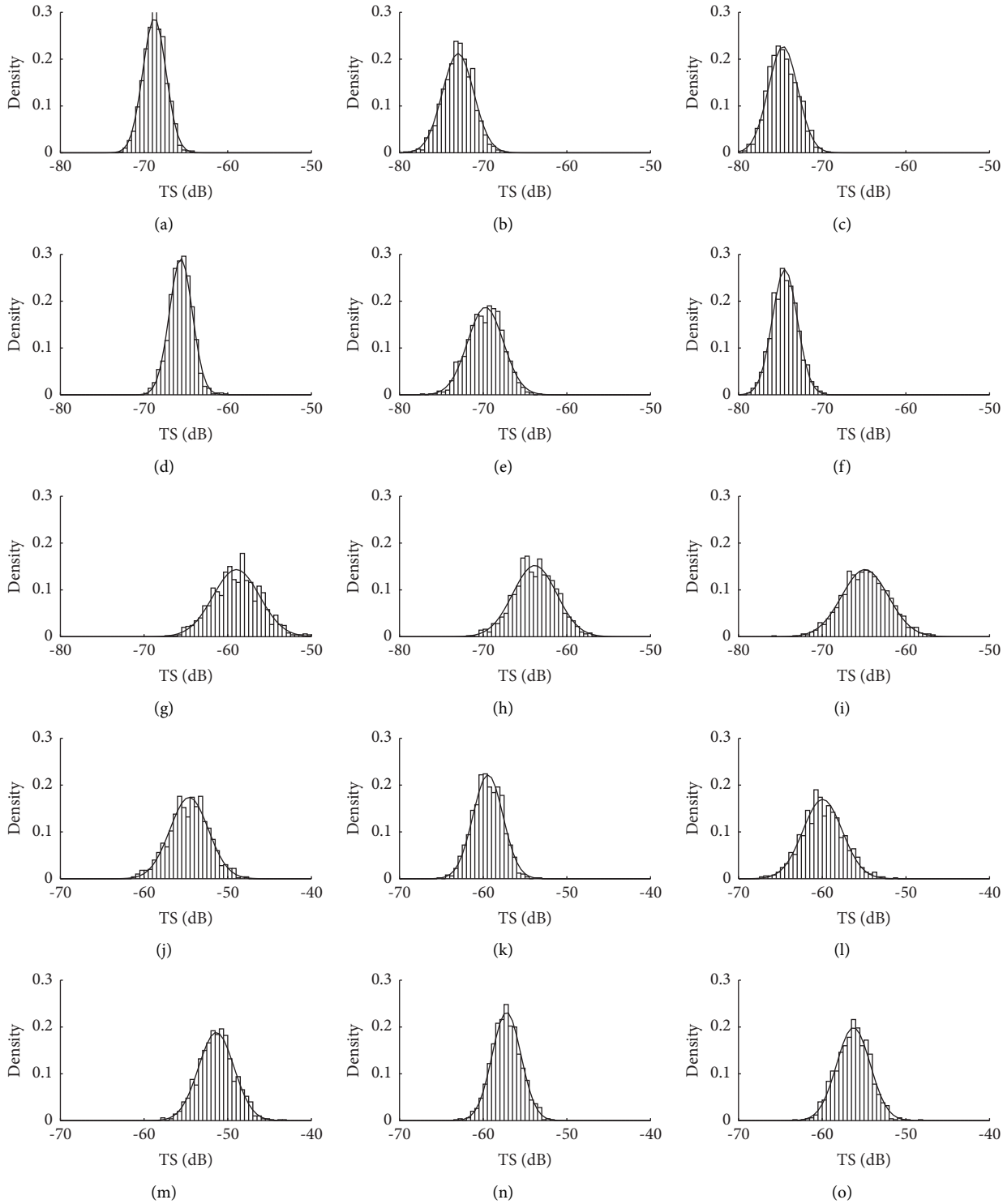

Figure 7: Histogram of resampled data for jellyfish TS in the horizontal swimming orientation at different frequencies. The caption of each subfigure is the number of the jellyfish sample-the center frequency of signals. The horizontal coordinate is the target strength, and the vertical coordinate is the probability density of the target strength measurements. (a) No. 1-70 kHz. (b) No. 1-120 kHz. (c) No. 1-200 kHz. (d) No. 2-70 kHz. (e) No. 2-120 kHz. (f) No. 2-200 kHz. (g) No. 3-70 kHz. (h) No. 3-120 kHz. (i) No. 3-200 kHz. (j) No. 4-70 kHz. (k) No. 4-120 kHz. (l) No. 4-200 kHz. (m) No. 5-70 kHz. (n) No. 5-120 kHz. (o) No. 5-200 kHz.

signals at multiple frequencies. The results show that the target strength of jellyfish swimming vertically is overall higher than that measured when swimming horizontally. The mean TS difference between the horizontal and vertical swimming orientation reached 5-6 dB. The difference in TS between individual jellyfish's horizontal and vertical

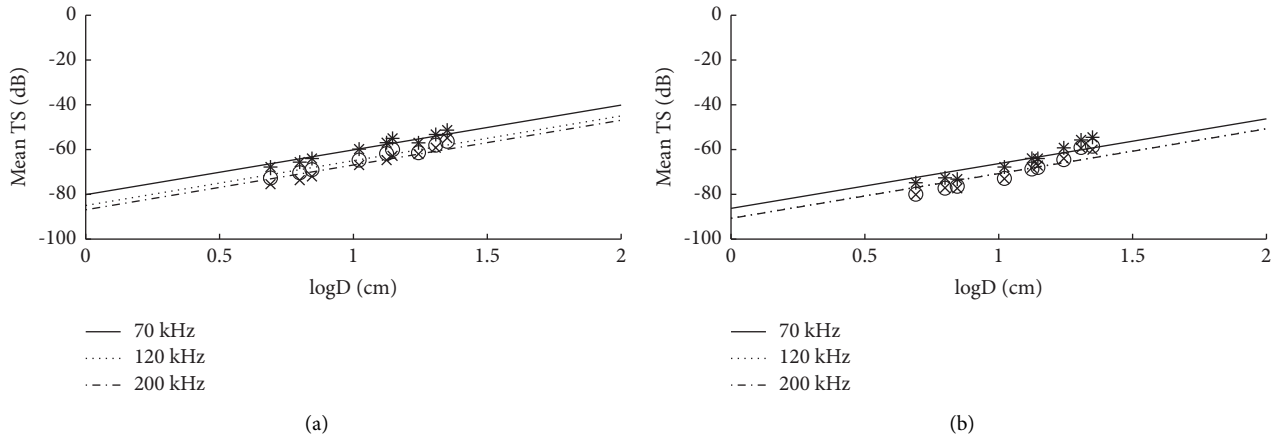

Figure 8: The relationship between mean TS and logarithmic diameter. The x-axis represents the logarithm of the bell diameter, while the y-axis represents the mean TS of the jellyfish sample. (a) The mean TS versus the logarithm of bell diameter for the vertical swimming orientation of the jellyfish. (b) The mean TS versus the logarithm of bell diameter for the horizontal swimming orientation of the jellyfish. The dots on the graph indicate the mean TS, where the black asterisk is the measured TS at 70 kHz, the black circle is the measured TS at 120 kHz, and the black cross is the measured TS at 200 kHz. The solid black line in the figure shows the predicted regression line for the measurement of a broadband signal with a center frequency of 70 kHz, the dashed black line in the figure shows the predicted regression line for the measurement of a broadband signal with a center frequency of 120 kHz, and the dotted black line in the figure shows the predicted regression line for the measurement of a broadband signal with a center frequency of 200 kHz.

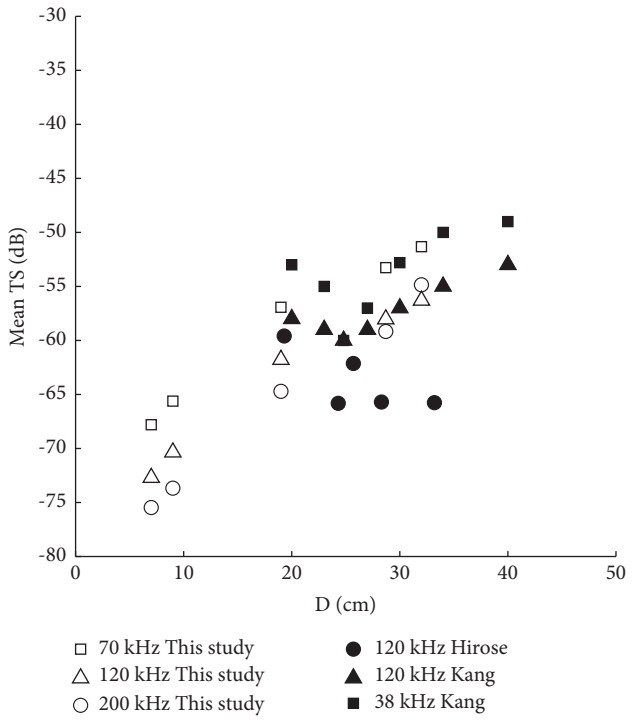

Figure 9: Relationship between jellyfish mean TS and bell diameter at different frequencies. Hollow squares: this study (70 kHz); hollow triangle: this study (120 kHz); hollow circles: this study (200 kHz); filled circles: Hirose et al. [31] (120 kHz); filled triangle: Kang et al. [30] (120 kHz); filled squares: Hirose et al. [31] (38 kHz).

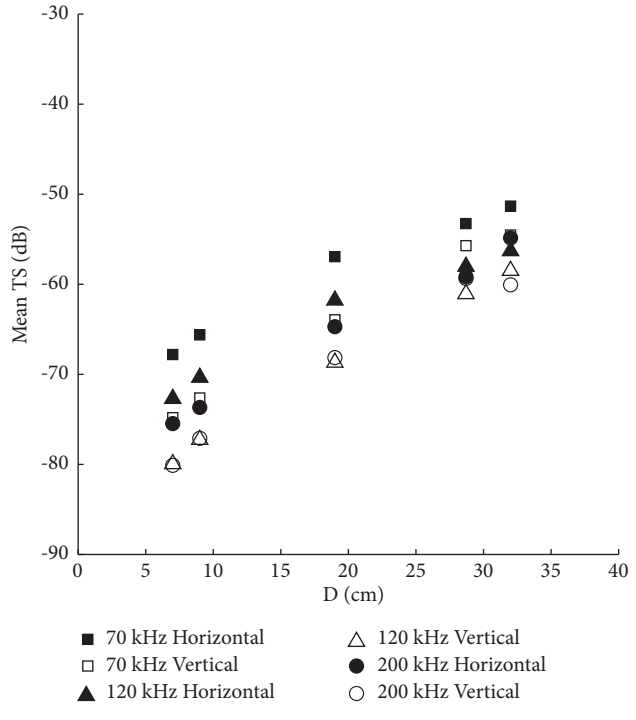

Figure 10: Jellyfish mean TS versus bell diameter for different swimming orientations at multiple frequencies. Filled squares: 70 kHz (horizontal); hollow squares: 70 kHz (vertical); filled triangle: 120 kHz (horizontal); hollow triangle: 120 kHz (vertical); filled circles: 200 kHz (horizontal); hollow circles: 200 kHz (vertical). The frequency indicated in the figure is the center frequency.

swimming orientation was 8–15 dB during the measurements. In general, one of the critical elements affecting TS measurements is thought to be jellyfish pulsation. When holding the measurement direction constant, Kang et al. demonstrated that the effect of individual jellyfish pulsation on TS was 4–15 dB [30]. Accordingly, it is evident that both jellyfish swimming orientation and jellyfish pulsation have a comparable effect on TS measurements. TS measurements

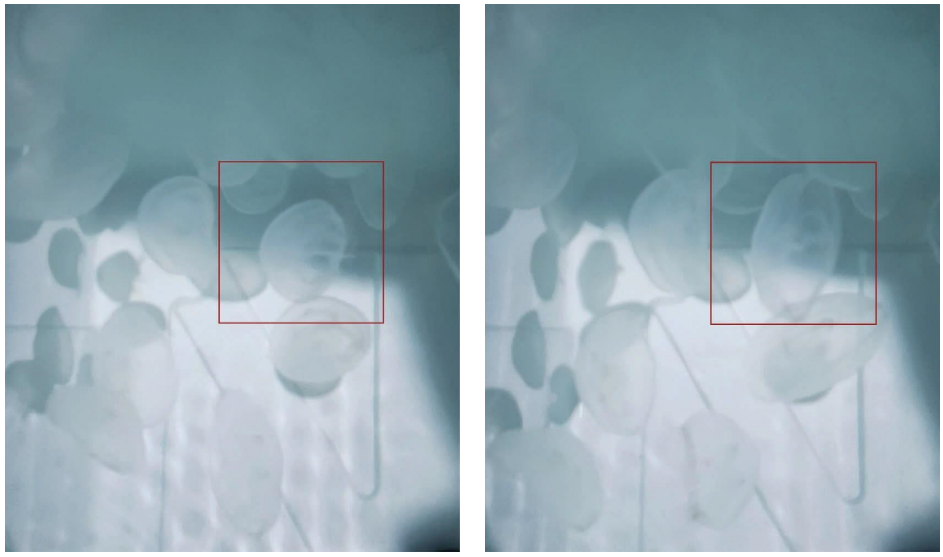

(a) (b)

Figure 11: Jellyfish group swimming posture. (a) Jellyfish in contracted state. (b) Jellyfish in diastolic state.

should consider jellyfish swimming orientation as well as other crucial elements.

Environmental factors such as currents may affect the specimens in the measurement of jellyfish TS. The water flow rate throughout the test may affect the TS by affecting the jellyfish's contraction and the jellyfish's movement posture. To test this hypothesis, we cultivated 200 *Aurelia aurita* jellyfish in four batches and tracked their swimming patterns. Figures 11(a) and 11(b) show the results of the video analysis of the swimming patterns while maintaining the salinity and temperature of the saltwater at the experimental levels. The frequency of jellyfish contraction movement was 24–30 times per minute in the state of flowing water, with almost 70% of the jellyfish maintaining swimming horizontally. In contrast, the frequency of contraction movement was significantly slower in the case of slow or no significant water flow, at 15–19 times per minute, comparable to the frequency of TS change measured by Kang et al. [30]. When the water stopped moving, the jellyfish's contractile motion slowed down even further, making it look like it was hanging in the air. These variations in contraction motion frequencies may have led to discrepancies in measurement results.

The final obtained TS values will be influenced by the jellyfish's swimming pattern and the frequency of its pulsation throughout the test. The jellyfish's swimming pattern and pulsation frequency are regulated by external environmental factors such as water currents, which are complex. We believe that the swimming pattern or distribution characteristics of the jellyfish population also have an important influence on the overall echo strength during the actual measurements. Notably, our proposed model does not account for the impact of current. To improve the accuracy of the jellyfish acoustic scattering model in the future, we believe it is worthwhile to investigate further the mechanism underlying the interaction between the jellyfish swimming orientation, pulsation, and environmental factors.

4. Conclusions

In conclusion, we obtained the TS of jellyfish *Nemopilema nomurai* in both horizontal and vertical swimming orientations for different center frequency broadband signals. The results show that broadband signal measurements are equally reliable in obtaining TS of jellyfish, similar to narrowband signals in terms of frequency differences, and that the contribution of jellyfish swimming attitude to the effect of TS measurements is comparable to the contribution of jellyfish pulsation motion to the effect of TS measurements. The results show significant differences in TS for different jellyfish swimming attitudes. We anticipate that the presented TS measurements and models for jellyfish horizontal swimming orientation can serve as a valuable reference to enhance the accuracy and precision of acoustic surveys of jellyfish *Nemopilema nomurai*. However, further research is well needed to explore the relationship between jellyfish swimming orientation, pulsating motion, and the external environment to achieve more accurate biomass estimates.

Data Availability

The TS data used to support the findings of this study are available from the corresponding author upon request.

Conflicts of Interest

The authors declare that there are no conflicts of interest regarding the publication of this paper.

Acknowledgments

We thank Yuhong Yang, Jiaming Wang, and Chongyang Sun for their help with the experiments. This research was supported by the National Natural Science Foundation of China (NSFC), China (grant number: 32073026), and the

Sanya Yazhou Bay Science and Technology City Administration, China (grant number: SKJC-2020-01-013).

References

[1] N. Henschke, "Jellyfishes in a changing ocean," in *Predicting Future Oceans*, pp. 137–148, Elsevier, Amsterdam, The Netherlands, 2019.

[2] Z. Dong, D. Liu, and J. K. Keesing, "Jellyfish blooms in China: dominant species, causes and consequences," *Marine Pollution Bulletin*, vol. 60, no. 7, pp. 954–963, 2010.

[3] S. Sun, X. X. Sun, and I. R. Jenkinson, "Preface: giant jellyfish blooms in Chinese waters," *Hydrobiologia*, vol. 754, pp. 1–11, 2015.

[4] J. Terenzini, Y. Li, and L. J. Falkenberg, "Unlocking Hong Kong's hidden jellyfish diversity with citizen science," *Regional Studies in Marine Science*, vol. 62, Article ID 102896, 2023.

[5] J. Song and L. Duan, "The yellow sea," in *World Seas: An Environmental Evaluation*, Elsevier, Amsterdam, The Netherlands, 2019.

[6] P. P. Wang, F. Zhang, and S. Sun, "Predation effect on copepods by the giant jellyfish Nemopilema nomurai during the early occurrence stage in May in the northern East China Sea and southern Yellow Sea, China," *Marine Pollution Bulletin*, vol. 186, Article ID 114462, 2023.

[7] S. I. Uye, "Blooms of the giant jellyfish Nemopilema nomurai: a threat to the fisheries sustainability of the East Asian Marginal Seas," *Plankton and Benthos Research*, vol. 3, pp. 125–131, 2008.

[8] B. Nastav, M. Malej, A. Malej, and A. Malej, "Is it possible to determine the economic impact of jellyfish outbreaks on fisheries? A case study–Slovenia," *Mediterranean Marine Science*, vol. 14, no. 1, pp. 214–223, 2013.

[9] M. Bosch-Belmar, E. Azzurro, K. Pulis et al., "Jellyfish blooms perception in Mediterranean finfish aquaculture," *Marine Policy*, vol. 76, pp. 1–7, 2017.

[10] A. J. Richardson, A. Bakun, G. C. Hays, and M. J. Gibbons, "The jellyfish joyride: causes, consequences and management responses to a more gelatinous future," *Trends in Ecology & Evolution*, vol. 24, no. 6, pp. 312–322, 2009.

[11] G. Vineetha, V. Kripa, K. K. Karati, N. Madhu, P. Anil, and M. Vishnu Nair, "Surge in the jellyfish population of a tropical monsoonal estuary: a boon or bane to its plankton community dynamics?" *Marine Pollution Bulletin*, vol. 182, Article ID 113951, 2022.

[12] S. H. Lee, L. C. Tseng, Y. Ho Yoon, E. Ramirez-Romero, J. S. Hwang, and J. Carlos Molinero, "The global spread of jellyfish hazards mirrors the pace of human imprint in the marine environment," *Environment International*, vol. 171, Article ID 107699, 2023.

[13] J. Shoji, T. Kudoh, H. Takatsuji, O. Kawaguchi, and A. Kasai, "Distribution of moon jellyfish Aurelia aurita in relation to summer hypoxia in Hiroshima Bay, Seto Inland Sea," *Estuarine, Coastal and Shelf Science*, vol. 86, no. 3, pp. 485–490, 2010.

[14] T. Kogovšek, M. Vodopivec, F. Raicich, S. I. Uye, and A. Malej, "Comparative analysis of the ecosystems in the northern Adriatic Sea and the Inland Sea of Japan: can anthropogenic pressures disclose jellyfish outbreaks?" *The Science of the Total Environment*, vol. 626, pp. 982–994, 2018.

[15] J. Castro-Gutiérrez, J. Gutiérrez-Estrada, J. Aroba et al., "Estimation of jellyfish abundance in the south-eastern Spanish coastline by using an explainable artificial intelligence model based on fuzzy logic," *Estuarine, Coastal and Shelf Science*, vol. 277, Article ID 108062, 2022.

[16] J. E. Purcell, "Jellyfish and ctenophore blooms coincide with human proliferations and environmental perturbations," *Annual Review of Marine Science*, vol. 4, no. 1, pp. 209–235, 2012.

[17] A. De Robertis and K. Taylor, "In situ target strength measurements of the scyphomedusa Chrysaora melanaster," *Fisheries Research*, vol. 153, pp. 18–23, 2014.

[18] L. C. Tseng, C. Chou, Q. C. Chen, and J. S. Hwang, "Jellyfish assemblages are related to interplay waters in the southern East China Sea," *Continental Shelf Research*, vol. 103, pp. 33–44, 2015.

[19] E. Eriksen, H. Gjøsæter, D. Prozorkevich et al., "From single species surveys towards monitoring of the Barents Sea ecosystem," *Progress in Oceanography*, vol. 166, pp. 4–14, 2018.

[20] D. G. Baker, T. D. Eddy, R. McIver et al., "Comparative analysis of different survey methods for monitoring fish assemblages in coastal habitats," *PeerJ*, vol. 4, Article ID e1832, 2016.

[21] S. A. Siddiqui, A. Salman, M. I. Malik et al., "Automatic fish species classification in underwater videos: exploiting pretrained deep neural network models to compensate for limited labelled data," *ICES Journal of Marine Science*, vol. 75, no. 1, pp. 374–389, 2018.

[22] K. M. Dunlop, T. Jarvis, K. J. Benoit-Bird et al., "Detection and characterisation of deep-sea benthopelagic animals from an autonomous underwater vehicle with a multibeam echosounder: a proof of concept and description of data-processing methods," *Deep Sea Research Part I: Oceanographic Research Papers*, vol. 134, pp. 64–79, 2018.

[23] J. Simmonds and D. N. MacLennan, *Fisheries Acoustics: Theory and Practice*, John Wiley & Sons, New York, NY, USA, 2008.

[24] G. Boyra, G. Moreno, B. Sobradillo, I. Pérez-Arjona, I. Sancristobal, and D. A. Demer, "Target strength of skipjack tuna (Katsuwanus pelamis) associated with fish aggregating devices (FADs)," *ICES Journal of Marine Science*, vol. 75, no. 5, pp. 1790–1802, 2018.

[25] V. Puig-Pons, P. Muñoz-Benavent, I. Pérez-Arjona et al., "Estimation of Bluefin Tuna (*Thunnus thynnus*) mean length in sea cages by acoustical means," *Applied Acoustics*, vol. 197, Article ID 108960, 2022.

[26] J. M. Jech, G. L. Lawson, and A. C. Lavery, "Wideband (15–260 kHz) acoustic volume backscattering spectra of Northern krill (Meganyctiphanes norvegica) and butterfish (*Peprilus triacanthus*)," *ICES Journal of Marine Science*, vol. 74, no. 8, pp. 2249–2261, 2017.

[27] J. M. Liu, H. Setiazi, and P. Y. So, "Fisheries hydroacoustic assessment: a bibliometric analysis and direction for future research towards a blue economy," *Regional Studies in Marine Science*, vol. 60, Article ID 102838, 2023.

[28] J. Dunning, T. Jansen, A. J. Fenwick, and P. G. Fernandes, "A new in-situ method to estimate fish target strength reveals high variability in broadband measurements," *Fisheries Research*, vol. 261, Article ID 106611, 2023.

[29] E. A. Yoon, D. J. Hwang, M. Hirose, E. H. Kim, T. Mukal, and B. S. Park, "Characteristics of acoustic scattering ac-cording to pulsation of the large jellyfish Nemopilema nomurai," *Korean Journal of Fisheries and Aquatic Sci-ences*, vol. 43, no. 5, pp. 551–556, 2010.

[30] D. Kang, J. Park, S. K. Jung, and S. Cho, "Estimates of acoustic target strength for giant jellyfish Nemopilema nomurai

Kishinouye in the coastal Northwest Pacific," *ICES Journal of Marine Science*, vol. 71, no. 3, pp. 597–603, 2014.
[31] M. Hirose, T. Mukai, D. Hwang, and K. Iida, "The acoustic characteristics of three jellyfish species: Nemopilema nomurai, Cyanea nozakii, and Aurelia aurita," *ICES Journal of Marine Science*, vol. 66, no. 6, pp. 1233–1237, 2009.
[32] D. J. Lee, H. Y. Kang, and M. S. Kwak, "Analysis and classification of broadband acoustic echoes from individual live fish using the pulse compression technique," *Korean Journal of Fisheries and Aquatic Sciences*, vol. 48, no. 2, pp. 207–220, 2015.
[33] C. Bassett, A. De Robertis, and C. D. Wilson, "Broadband echosounder measurements of the frequency response of fishes and euphausiids in the Gulf of Alaska," *ICES Journal of Marine Science*, vol. 75, no. 3, pp. 1131–1142, 2018.
[34] D. J. Lee, E. Kulubya, P. Goldin, A. Goodarzi, and F. Girgis, "Review of the neural oscillations underlying meditation," *Frontiers in Neuroscience*, vol. 12, pp. 178–186, 2018.
[35] S. Fossette, A. C. Gleiss, J. Chalumeau et al., "Current oriented swimming by jellyfish and its role in bloom maintenance," *Current Biology*, vol. 25, no. 3, pp. 342–347, 2015.
[36] W. M. Graham, S. Gelcich, K. L. Robinson et al., "Linking human well-being and jellyfish: ecosystem services, impacts, and societal responses," *Frontiers in Ecology and the Environment*, vol. 12, no. 9, pp. 515–523, 2014.
[37] E. A. Yoon, K. Lee, J. Chae et al., "Density estimates of moon jellyfish (Au-relia coerulea) in the Yeongsan estuary using nets and hydroacoustics," *Ocean Science Journal*, vol. 54, no. 3, pp. 457–465, 2019.
[38] T. R. Graham, J. T. Harvey, S. R. Benson, J. S. Renfree, and D. A. Demer, "The acoustic identification and enumeration of scyphozoan jellyfish, prey for leatherback sea turtles (Dermochelys coriacea), off central California," *ICES Journal of Marine Science*, vol. 67, no. 8, pp. 1739–1748, 2010.
[39] K. Amakasu and M. Furusawa, "The target strength of Antarctic krill (Euphausia superba) measured by the split-beam method in a small tank at 70 kHz," *ICES Journal of Marine Science*, vol. 63, no. 1, pp. 36–45, 2006.
[40] F. Bairstow, S. Gastauer, L. Finley et al., "Improving the accuracy of krill target strength using a shape catalog," *Frontiers in Marine Science*, vol. 8, p. 290, 2021.
[41] M. Hirose, T. Mukai, T. Shimura, J. Yamamoto, and K. Iida, "Measurements of specific density of and sound speed in Nomura's jellyfish Nemopilema nomurai to estimate their target strength using a theoretical scattering model," *J Marine Acoustical Society of Japan*, vol. 34, no. 2, pp. 109–118, 2007.
[42] D. A. Demer, L. Berger, M. Bernasconi et al., *Calibration of Acoustic Instruments*, International Council for the Exploration of the Sea (ICES), Europe, UK, 2015.
[43] R. J. Urick, *Principles of Underwater Sound*, McGraw-Hill, Uttar Pradesh, India, 1983.
[44] K. G. Foote, "Fish target strengths for use in echo integrator surveys," *Journal of the Acoustical Society of America*, vol. 82, no. 3, pp. 981–987, 1987.
[45] H. Shao, K. Minami, H. Shirakawa et al., "Target strength of a common kelp species, Saccharina japonica, measured using a quantitative echosounder in an indoor seawater tank," *Fisheries Research*, vol. 214, pp. 110–116, 2019.
[46] K. G. Foote, "On representing the length dependence of acoustic target strengths of fish," *Journal of the Fisheries Research Board of Canada*, vol. 36, no. 12, pp. 1490–1496, 1979.